Prediction for Complex Wing Planforms," *Journal of Aircraft*, Vol. 10, No. 6, 1973, pp. 379–381.

[4]Purvis, J. W., "Analytical Prediction of Vortex Lift," *Journal of Aircraft*, Vol. 18, No. 4, 1981, pp. 225–230.

[5]Kandil, O. A., Mook, D. T., and Nayfeh, A. H., "Nonlinear Prediction of Aerodynamic Loads on Lifting Surfaces," *Journal of Aircraft*, Vol. 13, No. 1, 1976, pp. 22–28.

[6]Carlson, H. W., and Mack, R. J., "Studies of Leading-Edge Thrust Phenomena," *Journal of Aircraft*, Vol. 17, No. 12, 1980, pp. 890–897.

[7]Kulfan, R. M., "Wing Airfoil Shape Effects on the Developments of Leading-Edge Vortices," AIAA Paper 79-1675, Aug. 1979.

[8]Kulfan, R. M., "Wing Geometry Effects on Leading-Edge Vortices," AIAA Paper 79-1872, Aug. 1979.

[9]Robinson, A., and Laurmann, J. A., *Wing Theory*, Cambridge Univ. Press, New York, 1956.

[10]Emerson, H. F., "Wind Tunnel Investigation of the Effect of Clipping the Tips of Triangular Wings of Different Thickness, Camber, and Aspect Ratio—Transonic Bump Method," NACA TN 3671, Dec. 1953.

[11]Er-El, J., and Yitzhak, Z., "Experimental Investigation of the Leading-Edge Suction Analogy," *Journal of Aircraft*, Vol. 25, No. 3, 1988, pp. 195–199.

Computational Study of Plume-Induced Separation on a Hypersonic Powered Model

L. D. Huebner*
NASA Langley Research Center, Hampton, Virginia 23681

Introduction

THE study discusses the computation of hypersonic airbreathing vehicle flowfields under simulated powered conditions. Specifically, this involves performing two-dimensional parabolized Navier-Stokes (PNS) and full Reynolds-averaged Navier-Stokes (RANS) calculations to predict the possible existence and effects of flow separation on the cowl of a hypersonic airbreathing model employing scramjet exhaust flow simulation at representative Mach 10 wind-tunnel conditions. This effect can occur at high enough values of the nozzle pressure ratio (NPR), defined as the ratio of the jet total to freestream pressure, where the plume developed from the internal nozzle expands into the aftbody region far enough away from the body that it causes a reverse flow in the boundary layer on the outside surface of the cowl (Fig. 1). This reverse flow can subsequently cause vortex formation and a separation of the boundary layer, which can be large enough to produce a separation-induced compression. Cowl flow separation under simulated powered conditions has been experimentally documented and computationally predicted.[1] However, its impact on model external aerodynamic forces and moments was not addressed. Flow separation near the cowl of a single expansion ramp nozzle was also predicted by Ruffin et al.,[2] but was said to have been caused by the curvature of the cowl near the trailing edge. Nevertheless, the separation could have been exacerbated by the presence of the plume.

Received June 8, 1993; revision received March 15, 1994; accepted for publication March 22, 1994.

*Aerospace Engineer, Hypersonic Airbreathing Propulsion Branch, Gas Dynamics Division, M/S 413. Senior Member AIAA.

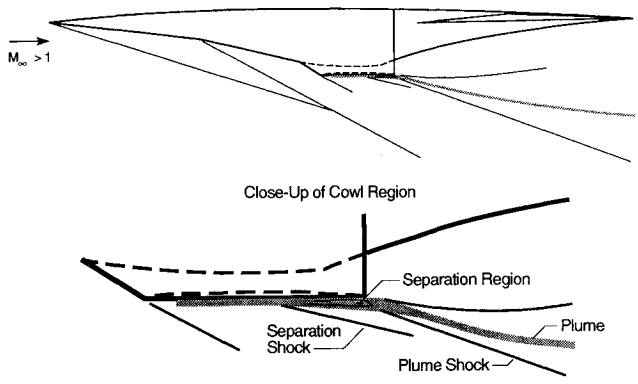

Fig. 1 Plume-induced separation phenomena.

It is the purpose of this Note to present the effects of plume-induced separation, in terms of flowfield features, surface pressures, and potential thermal concerns, using computational fluid dynamics (CFD).

General Aerodynamic Simulation Program 2.0 Attributes Employed

This study was part of a paper discussing the development of the CFD code known as the General Aerodynamic Simulation Program (GASP 2.0), which was the computational code used for this study.[3] Since this problem involves the possible existence and effects of cowl flow separation, both space marching (using the PNS equations) and global iterations (using the RANS equations) were performed independently. The PNS equations are not cast to predict streamwise separation; however, the RANS equations are able to predict streamwise separation. For this study a two-species chemistry model was created using the data base manager within GASP. This new model consisted of a mixture of two different perfect gases, one for the external flow (perfect gas air), and one for the internal flow (a perfect gas with a reduced ratio of specific heats and molecular weight corresponding to that of a non-combusting simulant gas used in powered hypersonic model wind-tunnel testing).[4] The multizone discretization was used to independently begin the external and internal flows and allow them to mix downstream.

Grid Details and Problem Initialization

The domain of the computational space is restricted to below the lower surface centerline of a generic hypersonic model. The geometry contains a faired-over inlet, similar to the type used in powered hypersonic wind-tunnel models. The effects of fairing over the inlet are extremely difficult to address experimentally, but a computational study was performed to assess the effects of inlet fairings.[5] The results of this fairing study showed only small surface pressure differences that were isolated to the region near the cowl leading edge, and that different fairings had little or no impact on lower surface aftbody pressures.

The computational forebody surface has an initial compression angle of 5 deg until the fairing begins about 27 cm downstream of the nose. The fairing adds about 10 deg of compression to the forebody flow. The flat cowl extends from the cowl leading edge (42.5 cm from the nose) to the cowl trailing edge, located about 53.5 cm from the nose. The initial nozzle expansion angle begins at the combustor exit and is approximately 20 deg. It transitions to a 10-deg expansion about halfway down the aftbody, which it maintains to the end of the vehicle, about 85 cm from the nose.

The three zones that comprise this grid are the internal nozzle zone, the forebody/inlet fairing/external cowl zone, and the aftbody zone (beyond the cowl trailing edge where the internal and external flows merge). Grid point connec-

tivity is maintained along zonal boundaries, as currently required by GASP 2.0.[3] The grid consisted of a total of 84,244 points. The grid was clustered near the body in all zones, with spacing appropriate for viscous calculations.

Two different flow conditions were of interest while performing the computations, namely, those that correspond to the wind-tunnel test conditions at freestream Mach numbers of 6 and 10. All information that pertains to the Mach 6 case can be found in Ref. 3, and the results are similar to those that will be presented here at Mach 10. The external flow was initialized with constant freestream conditions at the nose. For the Mach 10 problem, the external flow conditions included a freestream Reynolds number of 6.6×10^6/m, a freestream static temperature of 48.571 K, and a freestream density of 0.016905 kg/m^3. The internal flow was initialized at the nozzle throat of the model (beginning of the internal nozzle zone) with constant conditions spanning the nozzle height (i.e., boundary-layer profiles were not prescribed). The internal flow conditions included an NPR of 4000, a throat Mach number of 1.02, a jet total temperature of 3600 K, and an exhaust gas density of 1.25341 kg/m^3.

CFD Solution Issues

CFD solution issues pertaining to grid resolution and numerical convergence accuracy are discussed in detail in Ref. 3. Both the Mach 6 and Mach 10 PNS solutions were converged to four orders-of-magnitude residual reduction. These PNS solutions were then used as initial conditions for the RANS solutions. For the Mach 10 case, the RANS solution converged three orders of magnitude (beyond the four orders-of-magnitude PNS initial condition) in 3135 iterations. GASP performance results for this study include both time and memory requirements. In terms of computational time, the Mach 10 PNS solution took about 10 CPU min on a Cray-2, while the Mach 10 RANS solution used 2.75 CPU h. Memory requirements were 0.3 and 8.9 MWords for the Mach 10 PNS and RANS solutions, respectively.

Comparisons of PNS and RANS Solutions

Figure 2 shows a close-up of Mach number comparisons near the cowl for the Mach 10 PNS and RANS solutions. This figure reveals the details of the predicted separation region, as well as its impact on flowfield Mach numbers. The separated region creates an effectively larger boundary layer at the cowl trailing edge, resulting in an external plume shock that is displaced away from the body, as well as a different expansion pattern inside the plume and just beyond the cowl trailing edge. Furthermore, the concentration of contour lines at the cowl trailing edge and outside of the boundary layer denote the location of the separation-induced compression.

Integration of the pressures on the various parts of the lower surface also reveals differences caused by the formation of separated regions. Figure 3 shows pressure comparisons for the PNS and RANS solutions for the external lower surfaces at Mach 10. Two separation regions are actually predicted, one at the cowl trailing edge and one at the forebody compression ramp break. Table 1 summarizes these results in terms of forces and moments. The force and moment values are obtained by integrating differential pressures (per unit span) and taking the moment center about the expansion corner of the combustor exit. The forebody part begins at the nose and ends at the front of the cowl. The cowl piece is aligned with the freestream (thus contains no thrust contributions), and the aftbody part starts at the cowl trailing-edge plane and contains the rest of the lower surface. A number of comments can be made with respect to the data presented in Table 1. First, the separation on the forebody causes a small reduction in vehicle lift, thrust, and pitching moment. The cowl shows the largest force and moment variation of any part. The existence of the separation near the cowl trailing edge creates a higher pressure on the surface there. This force and moment variation is misleading when compared to the overall lower surface values, as will be discussed shortly. The aftbody force and moment differences are very small, indicating that the impact of cowl flow separation is minimal on the aftbody.

A more appropriate way of addressing the effect of cowl separation is made by studying the total lower-surface forces and moments, with and without cowl flow separation. The results are presented in Table 2. These results indicate that there are only small increments of lift and thrust caused by the separation, but there is a noticeable difference in pitching moment, which may be important in terms of trimming the vehicle.

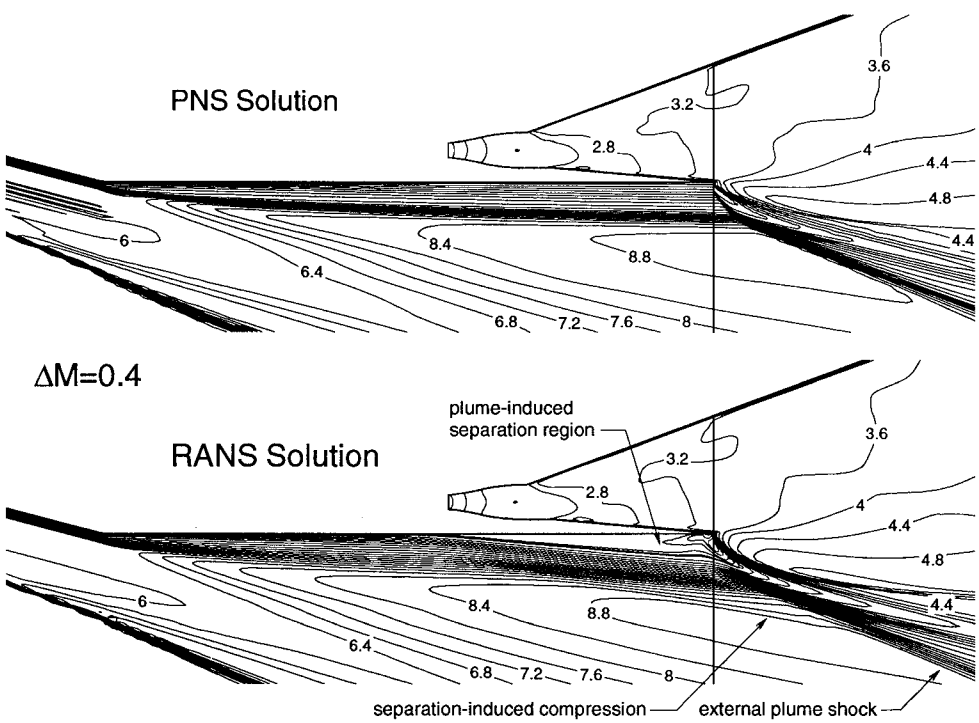

Fig. 2 Cowl-region Mach number contour comparison, PNS vs RANS solutions, $M_\infty = 10.0$, $Re_\infty = 6.6 \times 10^6$/m, NPR = 4000.

Table 1 Pressure integration summary for Mach 10 solutions

Part/solution	Lift, N/unit span	Thrust, N/unit span	Pitching moment, N-m/unit span
Forebody/PNS	16.9949	−3.8063	−3.4412
Forebody/RANS	16.6635	−3.6400	−3.3562
% Difference	−1.9	−4.4	−2.5
Cowl/PNS	0.7086	0.0000	−0.0335
Cowl/RANS	1.0155	0.0000	−0.0295
% Difference	+43.3	0.0	−11.9
Aftbody/PNS	32.5650	8.9916	4.6296
Aftbody/RANS	32.3684	8.9516	4.5823
% Difference	−0.6	−0.4	−1.0

Table 2 Total lower surface pressure integration for Mach 10 solutions

Total lower surface integrated pressures	Lift, lb/unit span	Thrust, lb/unit span	Pitching moment, in.-lb/unit span
With cowl separation	49.9371	5.3517	1.2399
Without cowl separation	50.0474	5.3116	1.1965
% Difference	+0.2	−0.7	−3.5

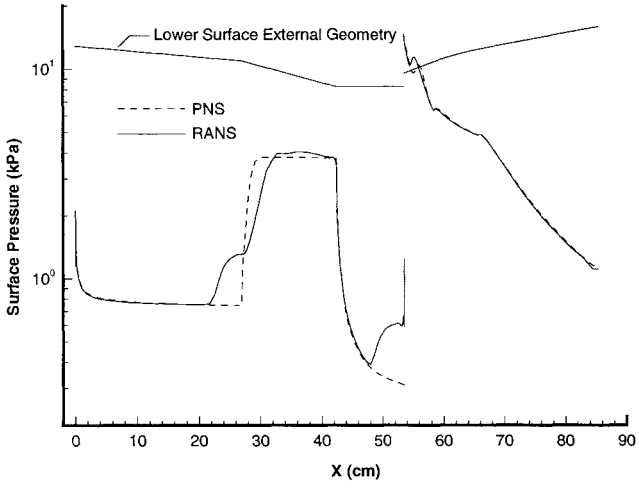

Fig. 3 Lower surface pressure comparison, PNS vs RANS solutions, M_∞ = 10.0, Re_∞ = 6.6 × 10^6/m, NPR = 4000.

Another concern about plume-induced flow separation is that high-temperature exhaust gas may actually be propagating upstream, causing increased thermal stress on the affected parts of the cowl. Plots of exhaust-gas mass fractions near the cowl trailing edge showed that the plume doesn't truly propagate upstream. Thus, it would not be expected that the external part of the cowl will require special cooling or material requirements to sustain the plume-induced separation behavior.

Conclusions

This study attempted to provide a better understanding of the possible existence and effects of plume-induced flow separation on the cowl of a hypersonic airbreathing vehicle employing scramjet exhaust flow simulation. For representative conditions at a freestream Mach number of 10, the results showed that flow separation was predicted on a generic configuration and resulted in a negligible difference in lift and thrust, while there was a small increase in pitching moment. For this configuration incorporating a flat cowl, no change in drag (negative thrust) was seen, but the results are likely geometry-dependent. If, e.g., the cowl trailing edge was at a position such that part of the cowl was an expansion surface, the separation would likely be greater, as would the impact on lift and thrust. It is further expected that the nature of the flow near the cowl trailing edge will preclude the plume from propagating forward and causing a region of thermal stress there.

References

[1]Huebner, L. D., and Tatum, K. E., "Computational and Experimental Aftbody Flow Fields for Hypersonic, Airbreathing Configurations with Scramjet Exhaust Flow Simulation," AIAA Paper 91-1709, June 1991.

[2]Ruffin, S. M., Venkatapathy, E., Keener, E. R., and Spaid, F. W., "Hypersonic Single Expansion Ramp Nozzle Simulations," *Journal of Spacecrafts and Rockets*, Vol. 29, No. 6, 1992, pp. 749–755.

[3]McGrory, W. D., Huebner, L. D., Slack, D. C., and Walters, R. W., "Development and Application of GASP 2.0," AIAA Paper 92-5067, Dec. 1992.

[4]Witte, D. W., Huebner, L. D., and Haynes, D. A., "A Test Technique for Using Metric Model Parts to Obtain Powered Effects on Airbreathing Configurations in Hypersonic Facilities," NASP TP 1008, Oct. 1993.

[5]Huebner, L. D., and Tatum, K. E., "Computational Effects of Inlet Representation on Powered Hypersonic, Airbreathing Models," *Journal of Aircraft*, Vol. 30, No. 5, 1993, pp. 571–577.

Effect of Leeward Flow Dividers on the Wing Rock of a Delta Wing

T. Terry Ng,* Tony Skaff,† and John Kountz†
University of Toledo, Toledo, Ohio 43606

I. Introduction

ONE of the limitations to combat effectiveness for all fighter aircraft is the phenomenon of wing rock. Attempts have been made in recent years on specific aircraft configurations[1,2] using a variety of both controls-oriented and aerodynamic fixes to control wing rock problems. Research efforts have been ongoing to understand the complexity of high-angle-of-attack vortex flows. Some examples of relatively recent studies aimed at understanding flows relating to wing rock are shown in Refs. 3–8. A significant number of these studies made use of the delta wing configuration.

Some of the aerodynamic phenomena that contribute to the wing rock of delta wings may play a part in the wing rock of a complete aircraft configuration. Of particular interest is the phenomenon of vortex position and breakdown asymmetry. During wing rock, large flow asymmetries are encountered on both the windward and leeward sides due to the changing sideslip. Large vortex asymmetries can be produced under this situation, thereby contributing to the building-up of wing rock amplitude.

Experimental studies on wing rock are inevitably affected by factors such as the particular model configuration, attachments of sensors and instrument, and model support arrangement. The specific technical objective of the present experimental study is to investigate the effect on wing rock of a symmetrically placed obstacle that deflects the leeward flow during sideslip conditions. The study was conducted on an 80-deg-sweep, sharp-edge delta wing because of the wealth of

Received Oct. 6, 1993; revision received March 9, 1994; accepted for publication March 11, 1994.

*Associate Professor, Department of Mechanical Engineering. Member AIAA.

†Graudate Student, Department of Mechanical Engineering.